

CYCLIC CRACK TIP DEFORMATION – THE INFLUENCE OF ENVIRONMENT

E. Gach and R. Pippan

Erich-Schmid-Institute of Materials Science,
Austrian Academy of Sciences, A-8700 Leoben, Jahnstraße 12

ABSTRACT:

Fatigue in metals is controlled by the cyclic plastic deformation at the crack tip. A simple direct observation of the crack tip deformation in the midsection of a specimen is not possible and the surface observation is usually not representative for the process along the crack front. We applied a stereophotogrammetric method to measure the real shape of the crack tip in the midsection of specimens. In this study the influence of ultrahigh-vacuum and a 3.5-% NaCl-solution on the crack growth behavior is reported. We determined both, the influence of environment on fatigue crack growth rate as well as the variation of the real shape of the crack tip in vacuum and saltwater in the midsection of a specimen. The examined materials were a cold-rolled austenitic stainless steel and an aluminum alloy 7020. It will be shown that the environment does not influence the cyclic crack tip opening displacement. The differences in crack growth rate are induced by changing of the shape of the crack tip during blunting.

KEYWORDS: cyclic crack tip deformation, environment, stereophotogrammetric method, crack growth rate

INTRODUCTION

A lot of different models, which try to explain the fatigue crack propagation behavior, can be found in the literature. These models are usually based on measured mean crack growth rate and (or) fractographic observations. However these experimental facts do not permit to decide which model describe the fatigue crack propagation behavior in a certain case. The only way to overcome this problem is to determine the deformation of the crack tip and the fracture processes directly. Such observations are not difficult at the surface, except in case of very small crack tip deformations. However the surface behavior is not representative for the deformation along the crack front, because the stress state in the vicinity of the crack tip at the surface differs from the midsection. In order to overcome this problem we have developed a special technique to determine the shape of the tip in the midsection of a specimen [1,2,3]. The aim of this paper is to investigate the effect of environment on the crack tip deformation and fatigue fracture process by direct observation in the midsection of the specimens.

MATERIAL AND ENVIRONMENT

Tests were performed in an austenitic stainless steel and an aluminum alloy 7020. The composition of this materials are shown in Tables 1 and 2. The fatigue crack growth tests were performed in ultrahigh-vacuum ($p < 10^{-7}$ Torr) and in 3.5-% NaCl-solution. The results were then compared with behavior in air.

The chosen ΔK was 70 and 20 $\text{MPa}\sqrt{\text{m}}$ in austenitic stainless steel and the aluminum alloy, respectively. The stress ratio R in both cases was 0.05.

TABLE 1:
Composition of the used austenitic stainless steel (weight-%).

El.	C	Cr	Ni	Mo	Si	Mn	P	S	W	Cu	Al	N
%	0.018	17.24	14.53	2.56	0.61	1.71	0.018	0.001	0.07	0.11	0.03	0.068

TABLE 2:
Composition of the aluminum alloy 7020 (weight-%)

El.	Al	Zn	Mg	Cr	Mn	Si	Zr	Fe
%	93.59	4.48	1.08	0.17	0.16	0.11	0.09	0.03

DEFORMATION BEHAVIOR IN AIR

Figure 1 a) shows the real shape of the crack tip in the midsection of specimen at maximum load in a constant amplitude test. The investigated material was a austenitic stainless steel, cycled at $\Delta K=70 \text{ MPa}\sqrt{\text{m}}$ and $R=0.05$. The determination of this 3D-image of the crack tip is shortly described later and for more details see [1,3,4,5].

Clearly visible are the striations on the fracture surface. The blue marked region, for example, corresponds to the striation which was formed in the last cycle. The red marked area is the blunting region which was formed during loading to the maximum load. In order to visualize what happens during a fatigue cycle the shape of the crack tip was determined at different loads [1,2]. From these images the crack tip opening displacement was easy to determine at different distances behind the crack tip during a load cycle, which is depicted in Figure 1 c). Figure 1 b) shows schematically the variation of the shape of the crack tip during one load cycle. At minimum load the crack tip is sharp. At a stress intensity of about 25 % of K_{max} the crack tip opens. The additional loading causes then a blunting of the crack. This blunting process continues till one reaches the maximum load. The shape of the crack looks like a V-notch. During unloading the crack resharpens, at first at the tip of the V-notch. At about 25 % the crack closes, which is also clearly visible in Figure 1 c), in the load vs. COD curve. From this observation we can see that the crack growth in air during loading by blunting (formation of a new fracture surface) and the unloading causes only a resharpening of the crack tip.

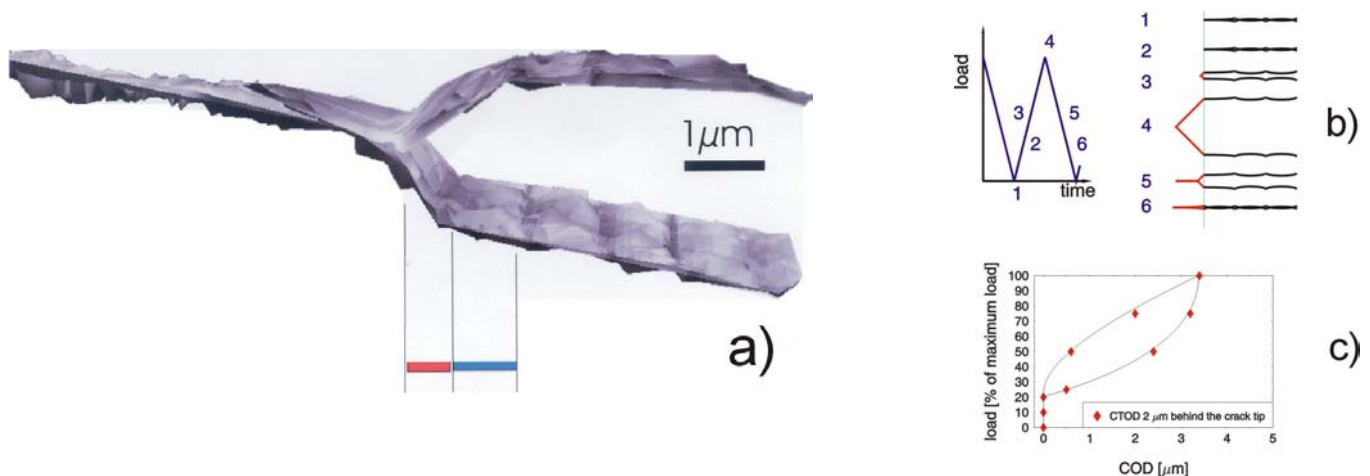


Figure 1: 3D-image of the shape of the crack tip in the midsection of the specimen at maximum load in a constant amplitude fatigue crack growth test ($\Delta K=70 \text{ MPa}\sqrt{\text{m}}$, $R=0.05$ – a)), the schematic crack tip deformation during a load cycle (b) and the variation of COD during a load cycle (c).

RESULTS AND DISCUSSION

Influence of environment on the crack growth rate

After failure of the specimen we observed the fracture surfaces in a scanning electron microscope. The crack extensions in different environments were clearly distinguishable. Hence, the crack growth rate could be determined.

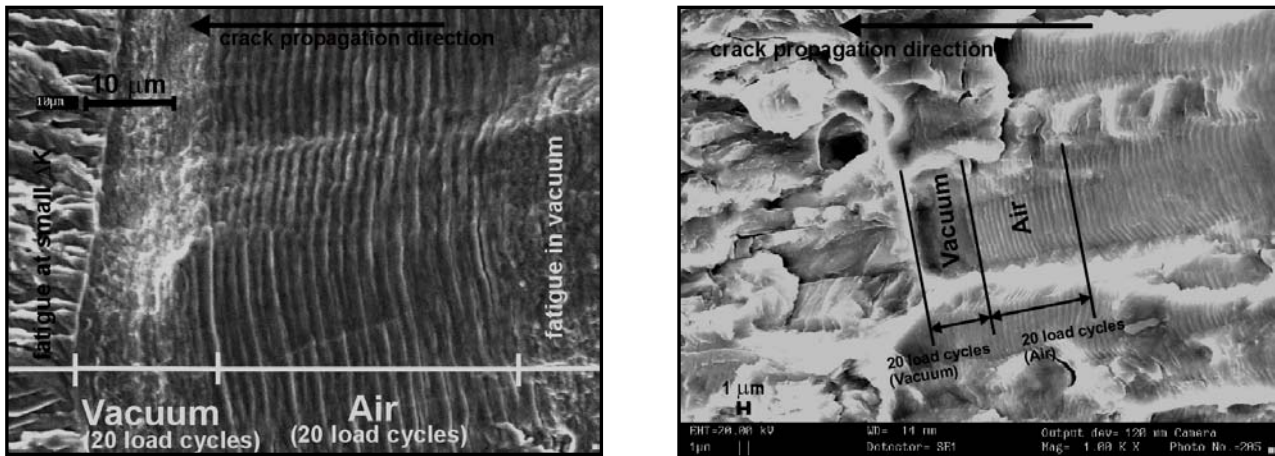


Figure 2: SEM-images from the fracture surface of an austenitic stainless steel (left) and an aluminum alloy 7020 (right). It shows a certain sequence of the constant amplitude test – approximately in the midsection of the specimen.

Figure 2 shows two SEM fractographs from a fatigue test. The fracture surface produced during 20 load cycles in air and 20 load cycles in vacuum at about 10^{-8} Torr is shown. In air clearly visible striations were formed at a constant load amplitude of $\Delta K=70 \text{ MPa}\sqrt{\text{m}}$ and a R-value of 0.05 in austenitic stainless steel, and $\Delta K=20 \text{ MPa}\sqrt{\text{m}}$ ($R=0.05$) in aluminum alloy 7020. By measuring the extensions of the crack produced in the different environments on the fracture surface and dividing through the number of load cycles we were able to calculate a mean value of the crack growth rate per cycle. In air we can control this result by determining the striation spacing at high magnifications in the SEM, because the width of one striation corresponds to the local crack growth rate da/dN . In the austenitic steel the crack growth in air is approximately two times larger than in vacuum. In the aluminum alloy 7020 the crack growth rate in air is roughly 2.30 times larger than in vacuum. In vacuum no striations were found. This result is well known from the literature. Pelloux have carried out experiments in aluminum alloys in vacuum and he also found no striations. He argued that the deformation in vacuum is more reversible as in air [6]. In air the new built fracture surface oxidize immediately and the formed oxide layer prevents a reversible deformation at the slip planes. As a result adjacent slip systems will be activated during unloading and one striations will be built [6]. Pelloux found that in aluminum alloys the crack growth rate in air is three times larger than in vacuum [6], which agrees relative good with our observations.

Influence of environment on the cyclic crack tip deformation

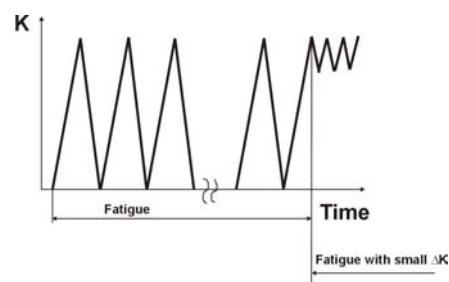


Figure 3: Experimental procedure to determine the crack tip deformation in the midsection of specimen at maximum load in a constant amplitude test.

For the determination of the cyclic crack tip deformation in the midsection of a specimen our fatigue test was interrupted at a chosen load, in this particular case at maximum load. Then a constant amplitude sequence with very small load amplitude was applied till the specimen failed. This small cyclic loading was used to fracture the specimen without changing the shape of the crack tip. Then the corresponding crack tip regions of both broken specimen halves were reconstructed. This was done by analyzing stereoscopic electron images of the two halves with an automatic image processing system [1,2,3]. Therefore we made an image from the fracture surface region and then an image from the same region of the tilted specimen. The tilting angle was 5 degree. We did that for both specimen halves. With an image processing system we got a three-dimensional model of both fracture surfaces. Now we were able to lay together the two 3D-models as in Figure 1 a) or to determine the height profiles along two corresponding lines. Fitting together the two corresponding height profiles give us the real shape of the crack tip. Figure 4 and 5 show two examples:

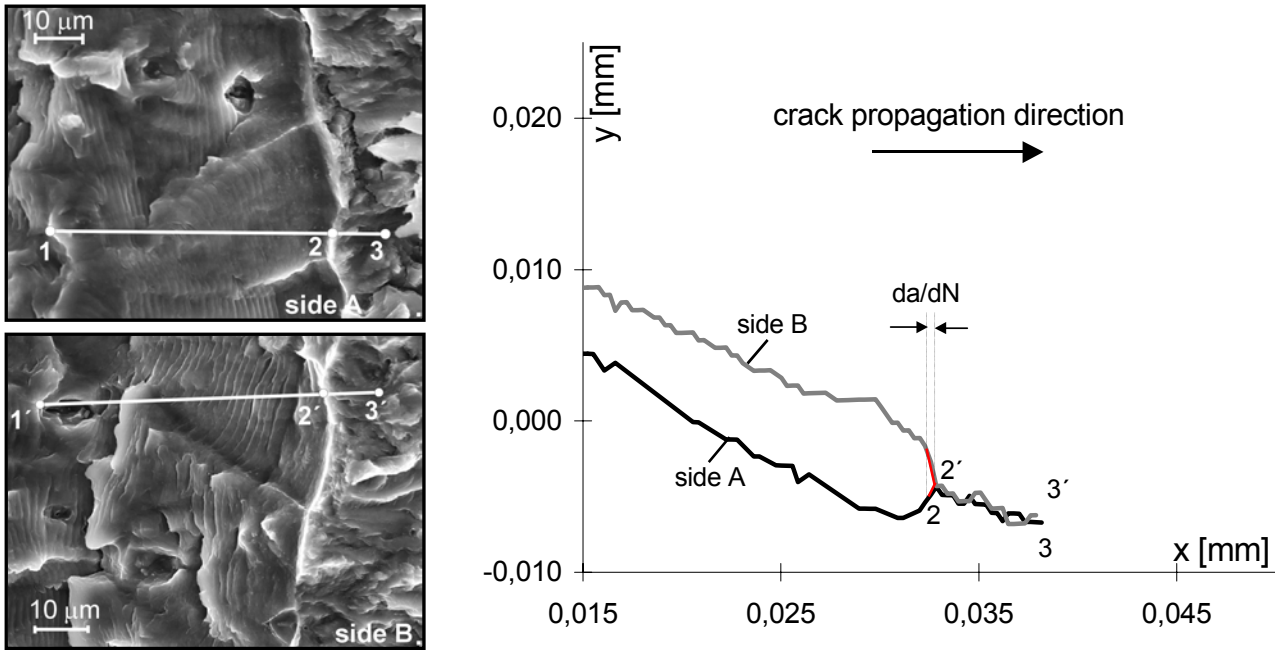


Figure 4: SEM-image from two corresponding fracture surfaces (aluminum alloy 7020) on both specimen halves. The determined height profiles gives the shape of the crack tip at the maximum load in vacuum.

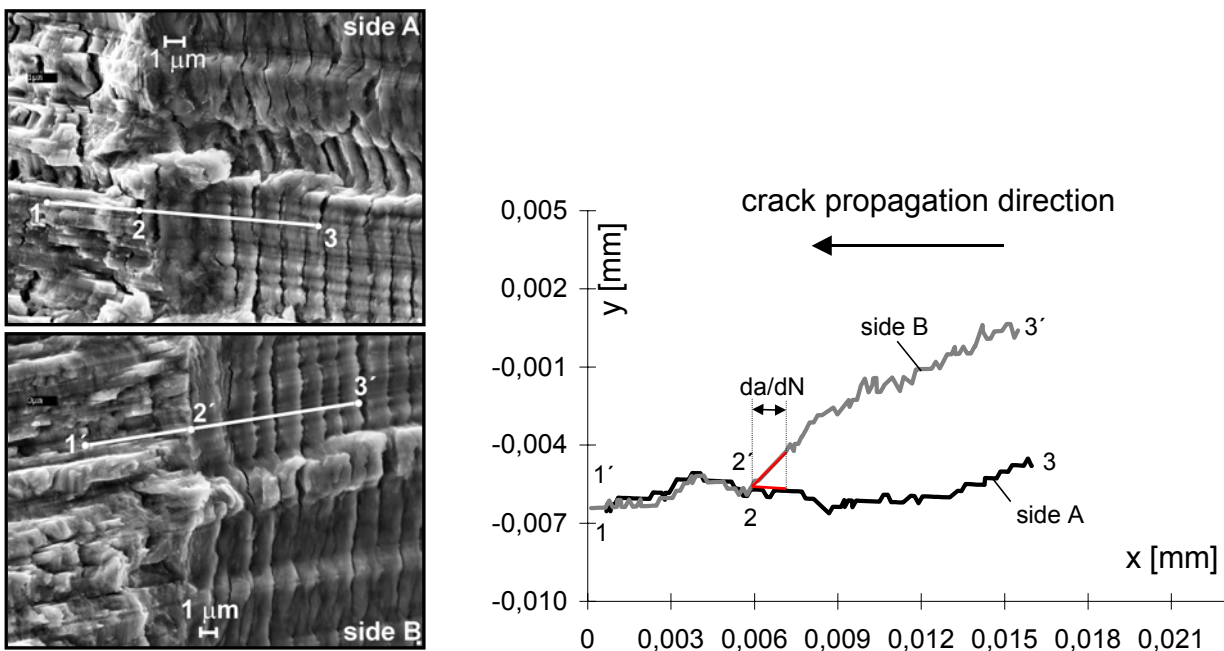


Figure 5: SEM-image from two corresponding fracture surfaces (austenitic stainless steel) on both specimen halves. The determined height profiles along the indicated line shows the shape of the crack tip at the maximum load in 3.5-% NaCl-solution.

Table 3 and 4 summarizes the results from the performed crack growth rate measurements and characteristic values from the determined shape of the crack tip in different environments, for both examined materials.

TABLE 3:

Crack tip opening displacement (CTOD) 3 and 7 μm behind the crack tip, crack tip opening angle (CTOA) or blunting angle, crack growth rate and relative crack growth rate for the austenitic stainless steel ($\Delta K=70 \text{ MPa}\sqrt{\text{m}}$, $R=0.05$) in different environments.

medium	CTOD 3 μm behind crack tip	CTOD 7 μm behind crack tip	CTOA	crack growth rate da/dN [$\mu\text{m}/\text{loadcycle}$]	Relative crack growth rate (vacuum as reference medium)
vacuum	4.30	4.60	$\approx 105^\circ$	0.50	1.00
air	3.30	4.30	$\approx 90^\circ$	1.00	2.00
saltwater	3.50	4.70	$\approx 60^\circ$	1.10	2.20

TABLE 4:

Crack tip opening displacement (CTOD) 3 and 7 μm behind the crack tip, crack tip opening angle (CTOA) or blunting angle, crack growth rate and relative crack growth rate for aluminum alloy 7020 ($\Delta K=20 \text{ MPa}\sqrt{\text{m}}$, $R=0.05$) in different environments.

medium	CTOD 3 μm behind crack tip	CTOD 7 μm behind crack tip	CTOA	crack growth rate da/dN [$\mu\text{m}/\text{loadcycle}$]	Relative crack growth rate (vacuum as reference medium)
vacuum	4.00	5.00	$\approx 130^\circ$	0.30	1.00
air	3.30	4.30	$\approx 90^\circ$	0.70	2.30
saltwater	3.90	4.70	$\approx 20^\circ$	1.70	5.70

It is evident from the depicted shapes of the crack tip and their determined characteristic values that the environment changes only the shape of the crack tip. The crack tip opening displacement at larger distances behind the crack tip remains constant. The determined differences are typical values for the scatter, which may be caused by small differences in the applied stress intensity range, real acting local stress intensity range in the investigated location or a small variation of the yield stress. A variation of crack closure stress intensity would also change crack tip opening displacement, however at this large ΔK , where only plasticity induced closure is important, this effect does not play a role. The effect of vacuum in both alloys is approximately the same. In vacuum the crack tip opening angle increases (or in other words, the shape of the crack tip changes from a V-shape notch to a more blunted notch). The effect of the NaCl-solution is also the same, however in the aluminum alloy the decrease in crack tip opening angle is much larger and hence also the increase in the crack growth rate is much larger.

CONCLUSIONS

Figure 6 shows a schematic summary of the crack tip deformation and the change of the relations between the crack growth rate (da/dN), the crack tip opening angle (CTOA) and crack opening displacement (COD) in the different environments.

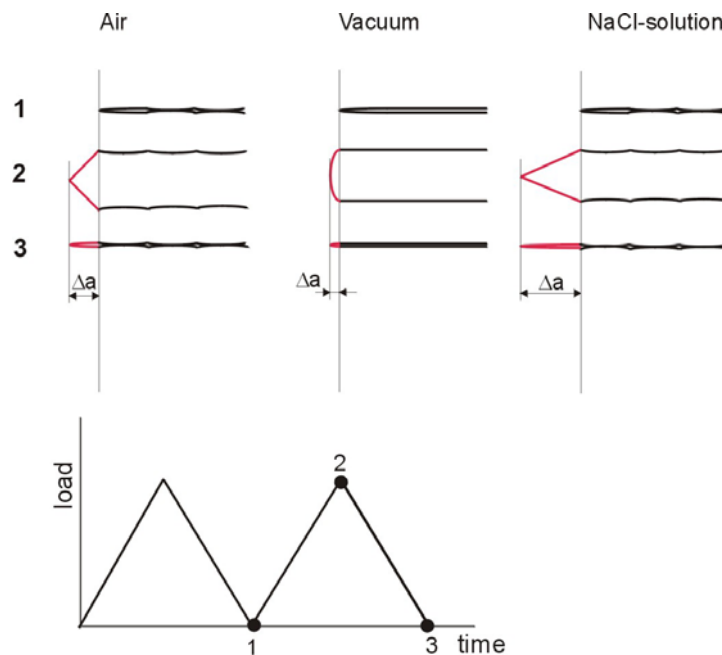


Figure 6: Schematic presentation of the shape of the crack tip at maximum load in different environments.

In all cases the crack propagation mechanism seems to be the same. It is a blunting and resharping mechanism. However the environment significantly changes the shape of the crack tip during the blunting.

- In vacuum it seems that blunting, with a relative large crack tip opening angle and a relative small crack extension can be occurred.
- In air the blunting or crack tip opening angle decreases, which may be induced by a fracture of the oxide layer or nano fracture of volume elements immediately in front of the tip of crack (tip of the V-notch). This induces the increase in the crack growth rate. The effect is similar in both alloys.
- In 3.5-% NaCl-solution this additional “fracture” at the crack tip of the notch increases, which induces an decrease of the crack tip opening angle and an increase of the crack extension during blunting. In austenitic stainless steel this effect was relative small and very large in aluminum alloy.

REFERENCES

1. Bichler, C. and Pippan, R., Direct Observation of the Formation of Striations, *Proc. Engineering against fatigue* (J.H. Beynon, M.W. Brown, T.C. Lindley, R.A. Smith & B. Tomkins), pp. 211-218.
2. Bichler, C., *Thesis*, University Leoben, 1997
3. Siegmund, Th., Kolednik, O. and Pippan R., Direct Measurement of the Cyclic Crack-Tip Deformation, *Zeitschrift für Metallkunde*, Vol. 81, (1990) pp. 677 –683.
4. Stampf, J., Scherer, S., Berchtaler, M., Gruber, M. and Kolednik, O., *International Journal of Fracture*, Vol. 78, 1996, pp. 35-44.
5. Kolednik, O., *Practical Metallogr.*, Vol. 18, 1981, pp. 562-573.
6. Pelloux, R.M.N., Mechanism of formation of ductile fatigue striations, *Trans. ASM* 62 (1969) 281-285.